Journal of Sciences, Islamic Republic of Iran 28(2): 113 - 118 (2017) http://jsciences.ut.ac.ir
University of Tehran, ISSN 1016-1104

Green Synthesis and Characterization of Bi_2O_3 Nanorods as Catalyst for Aromatization of 1,4-Dihydropyridines

F. Farzaneh*, L. Jafari Foruzin, Z. Sharif, and E. Rashtizadeh

Department of Chemistry, Faculty of Physics and Chemistry, Alzahra University, Vanak, Tehran, Islamic Republic of Iran

Received: 13 April 2016/ Revised: 26 September 2016/ Accepted: 5 November 2016

Abstract

Bismuth oxide (Bi_2O_3) nanorods was prepared via one pot sol-gel method using Bi(NO3)3.5H2O and starch (as template) in water under hydrothermal condition followed by calcination at 320˚C within 3 h. The resultant solid product was characterized by scanning electron microscope (SEM), X-ray diffraction (XRD), thermogravimetry (TGA), and FTIR techniques. Based on the obtained results, the formation of Bi_2O_3 nanoparticles and nanorods at lower and higher percentage of starch is promising. It was found that Bi_2O_3 nanorods catalyse the aromatization of 1,4-dihydropyridines (DHPs) with 100% conversion and 100% selectivity.

Keywords: Bi2O3 nanstructures; Hydrothermal synthesis; Aromatization; 1,4dihydropyridines.

Introduction

Over the past few years, considerable interest has been focused on the synthesis of nanostructures with controllable morphologies because of the strong relationship between the structures and their attractive physical or chemical properties [1]. Due to the unique structural and surface properties, inorganic three-dimensional (3D) spherical structures with nanometer to micrometer size are proposed to have potential applications in catalysis, chemical sensors, photo catalysis, controlled delivery and release of drugs [1]. Bi_2O_3 is an important p-type semiconductor with four main crystallographic polymorphs denoted as α-, β-, γ -, and δ-Bi_2O_3 [2]. Bi_2O_3 has received considerable attention because of its various applications such as photo catalyst [3], solid oxide fuel cell [4], gas sensor [2] and catalyst for oxidation of hydrocarbons [5]. Several methods have been used for preparation of Bi_2O_3 nanoparticles such as microwave-assisted synthesis [6, 7], electrodeposition route [8], thermal oxidation [9], thermal plasma and heat treatment [10], laser ablation [11] and chemical vapour deposition (CVD) [12].

Dihydropyridines (DHPs) are analogues of nicotinamide adenosine dinucleotide hydride (NADH). The 1,4-DHP present in coenzymes NADH and NADPH mediates hydrogen-transfer reactions in biological systems [13]. It has been found that NADH initially undergoes oxidative aromatization to the corresponding pyridine derivative during the metabolism by the action of cytochrome P-450 present in liver [14]. In order to understand these biological processes, as well as to develop a useful synthetic approach to poly substituted pyridines, the oxidative aromatization of 1, 4- dihydropyridine (DHP) derivatives has received considerable attention from synthetic chemists [15]. Numerous methods for the aromatization of 1,4-DHPs have been developed for that purpose including the use of metallic salts, non-metallic

* Corresponding author: Tel: +982188041344; Fax: +9802188041344; Email: faezeh_farzaneh@yahoo.com, farzaneh@alzahra.ac.ir

reagents, catalytic methods [16]. Dihydropyridines have been aromatized to pyridines by various reagents such as SiO_2-$VO(OH)_2$ [17], K_2CO_3 [18], silica supported cobalt catalysis[19], Vanadium-Substituted Wells-Dawson heteropolyacid [20], Si-Zr-Mo [21], H_2O_2/NaI[22], $MoOCl_4$ and $MoCl_5$ [23] and radical cation salts [24].

Herein, we report the one-pot, sol-gel synthesis and characterization of Bi_2O_3 nanorods in water and using it as catalyst for oxidative aromatization of Hantzsch 1,4-DHPs to the corresponding substituted pyridines.

Materials and Methods

Materials and Instrumentation Details

Starch, Bismuth nitrate $Bi(NO_3)_3{\cdot}5H_2O$, nitric acid (65%), ethanol, benzaldehyde, ethyl acetoacetate and ammonium acetate were purchased from Merck Chemical Company and used without further purification. X-ray powder diffraction (XRD) data were recorded on a diffractometer type, (Philips PW1800) at room temperature, operating at 40 kV and 30 mA, using Cu kα_1 radiation (λ = 1.5406 Å). The nanostructures of the sample were analysed by scanning electron microscope (SEM, S-4160 Hitachi), thermal studies were performed using Mettler-Toledo TGA/SDTA-851 at heating rate of 25ºC/min, under oxygen atmosphere. FT-IR spectra were recorded on a Bruker Tensor 27 FTIR spectrometer with KBr powder and UV spectra measured on Perkin Elmer Lambda 35, double beam spectrophotometer. Oxidative aromatization products were analyzed by GC and GC-MS using an Agilent 6890 Series with FID detector, HP-5, 5% phenyl methyl siloxane capillary and an Agilent 5973 network, mass selective detector, HP-5 MS 6989 Network GC system, respectively.

Preparation Bi_2O_3 nanoparticles

Bismuth nitrate (4.2 mmol, 2 g) was dissolved in 10 mL nitric acid solution (65% in 20 mL water,). After formation of a clear solution, desired amount of starch was added and the mixture stirred for 1h in 90ºC using a water bath. The solution was then transferred into a Teflon-lined stainless steel reaction autoclave followed by heating at 100˚C for 48 h. After cooling to room temperature, the mixture was centrifuged, filtered, washed with deionised water and then dried at room temperature. Subsequent calcination of the solid at 320˚ C for 3 hours finally afforded the nanostructured Bi_2O_3.

Synthesis of 1,4 dihydropyridines (1, 4-DHPs)

1,4-DHPs was prepared as reported [25]. A 10 mL round-bottom flask was charged with ethyl acetoacetate (2 mmol), aldehyde (benzaldehyde, formaldehyde, acetaldehyde, 1mmol) and ammonium acetate (1.5 mmol) and stirred under solvent-free conditions. The reaction was completed within 0.25–4.5 hours at 80 °C. The crude product was isolated by precipitation upon addition of cooled water followed by vigorous shaking and decanting the aqueous layer. The residue was then dissolved in a suitable solvent and dried with anhydrous Na_2SO_4. After evaporation of the solvent under reduced pressure, 1,4-DHPs were obtained and used without further purification.

Oxidative aromatization of Hantasch 1,4-DHPs with Bi_2O_3

A stirring suspension of 1,4-DHP (0.06 mmol) and Bi_2O_3 nanorods (10 mg) in ethanol (15 mL) was heated at reflux for 6 h. After completion of the reaction as indicated by TLC, the mixture was poured into H_2O (10 mL) and extracted with CH_2Cl_2. The organic layer was dried with anhydrous Na_2SO_4. The product was analysed with GC and GC-MS techniques.

Results and Discussion

Characteristics of Bi_2O_3 nanoparticles

Bi_2O_3 nanoparticles and nanorods were prepared from bismuth nitrate in water using 23.1% and 53.4% starch as template respectively.

The XRD patterns of Bi_2O_3 nanorods before and after calcination are shown in Figure1a, b respectively. As seen in the XRD pattern of the prepared Bi-Starch hybrid (Figure 1.a) the characteristic peaks with d values of 5.32, 4.24, 3.97, 2.97 and 2.66 are related to the starch [26], the remaining peaks consistent with JPCDS card no. 044-1246 are related to Bi specioes (trigonal with Space group : R-3m) in hybrid. The XRD pattern of calcined sample at 320˚ C consistent with JCPD standard card no (27- 0050) indicates the formation of tetragonal β-Bi_2O_3 [27]. The XRD pattern of Bi_2O_3 nanoparticles is similar to the nanoroads in which indicated the formation of tetragonal β-Bi_2O_3.

The FTIR spectra of Starch, $BiNO_3.5H_2O$, Bi-Starch Hybrid before and after calcination at 300ºC and reused catalytst are shown in Figure 2 (a-e) respectively. The appeared two peaks centered at 1385 and 1170 cm^{-1} are attributed to the C-O vibrations of starch (Figure 2- a) [28]. Two rather medium peaks observed at 600-500 cm^{-1} in the FTIR spectrum of the precursor are attibuted to the vibration of Bi-O [29] and a band appearing at 880 cm^{-1} is attributed to the C-O-Bi vibration in the hybride formation step (Figure 1c). After calcination two new peaks appeared at 550 and 600 cm^{-1} due to the Bi-O vibrations (Figure1d) [30]. Particularly significant is the similarity observed in the FTIR spectra of nano

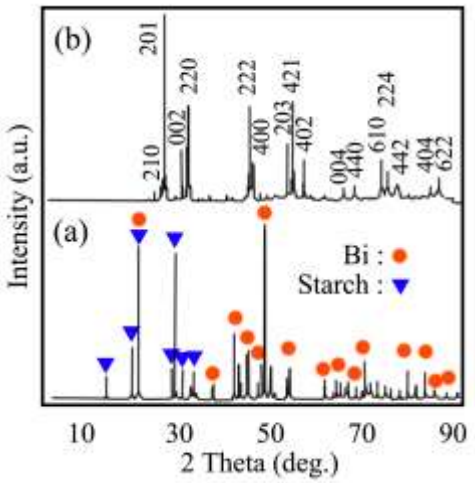

Figure 1. The XRD patterns of (a) hybrid Bi-starch and (b) nano Bi_2O_3.

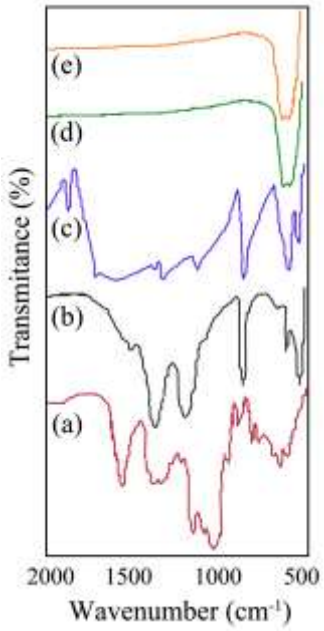

Figure 2. The FT-IR specra of (a) starch (b) $BiNO_3.5H_2O$, (c) hybrid Bi-Starch, (d) after calcination at 300ºC, (e) reused as catalytst.

Bi_2O_3 before and after using as catalyst (Figure 1 e).

In order to investigate the appropriate calcination temperature for transformation of hybrid to Bi_2O_3, the TGA was conducted under free atmosphere. The obtained results as well as the corresponding differential thermo analysis DTA curves are shown in Figure 3a,b respectively. Three parts consisting the approximate weight losses of 0.4%, 26% and 1.41% at 150°, 320ºC and 310° to 650°C due to the adsorbed water evaporation, starch template decomposition, and

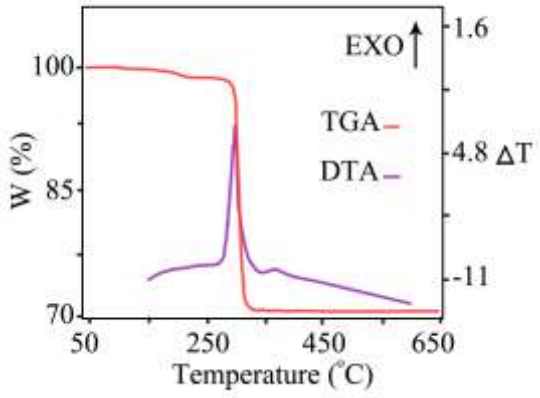

Figure 3. The TGA-DTA of nano hybrid Bi-starch.

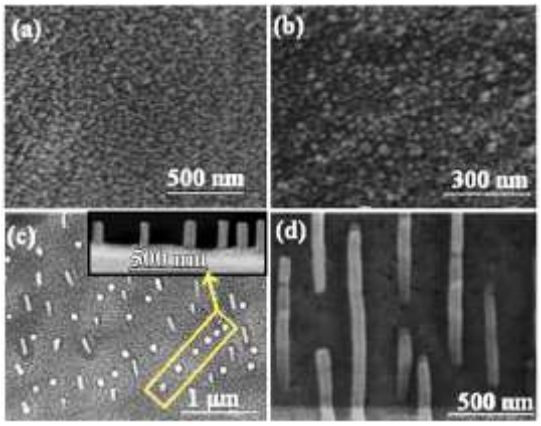

Figure 4. Scanning electron microscopy of (a,b) hybrid Bi-starch with 0.6g starch, before and after calcination, (c,d) with 2,2 g starch before and after calcination.

complete decomposition of template, respectively are evident in TGA analyses data. The DTA curve indicating an exothermic peak located around 300°C exhibits the template decomposition temperature [31]. The observed exothermic peaks in the range 300°-400°C in the DTA curve is assigned to the exothermic starch combustion.

Typical SEM images of the prepared Bi salt and starch hybrid designated as precursor sample containing starch 23.1% (0.6 g) and 53.4% (2.2 g) before and after calcination are shown in Figures 4a-b and 4c-d, respectivly. Before (Figure 4a) and after calcination (the hybrid with 0.6g starch) (Figure 4b), the formation of nanoparticles wih particle size of 50- 80 nm is evident. By increasing the amount of starch to 2.2 g , a change in the morphology from spherical to nanorods is observed. As seen in Figure 4c, whereas the sample is nanorods before calcination, more similar nanorods sample

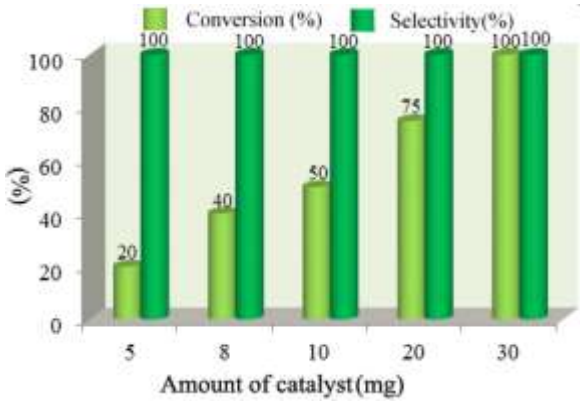

Figure 5. The effect of amount of catalyst on aromatization of 1,4-DHP.

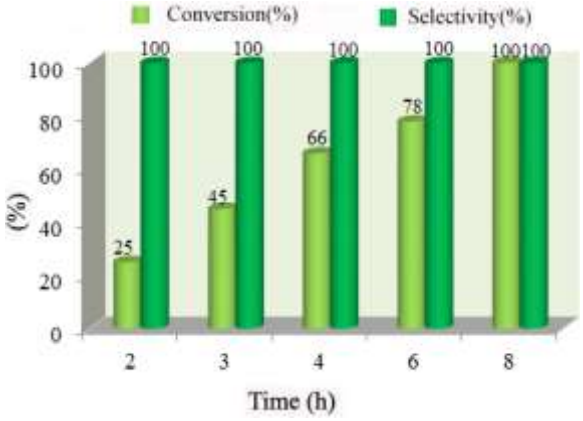

Figure 6. The effect of time on aromatization 1,4-DHP.

aligned to each other with approximate diameter of 50 nm is formed after calcination (Figure 4d).

Catalytic dehydrogenation of DHPs

The prepared nanoparticles and nanorods were found to successfully catalyse the Hantzsch aromatization of 1,4-DHPs. The effect of the amount of catalyst and time on aromatization of 1,4 dihydro-4-phenyl-2,6 dimethyl-3,5 pyridinedicarboxylate designated as 1,4-DHP as representative model are shown in Figures 5 and 6 respectively. Whereas quantitative aromatization was observed in the presence of 30 mg of the catalyst within 8 h (Figure 5), conversions were partially proceeded during 2 or 8 h (Figure 6). Therefore, other DHP aromatizations were investigated under optimized reaction conditions. As indicated in Table 1 (entries 2, 4, 6), for R=H, R= CH_3 and R= Ph have proceeded within 4, 6 and 8 h (with 30mg catalyst), conversion and selectivity were 100%. As indicated in this Table the optimum time for using 15 mg catalyst were also reported (entries 1, 3, 5, Table 1). The observed rate decreasing trend when R is Ph (entry 5, Table 1) is in accord with the increasing steric hindrance at the substituted carbon. The ^{1}H-NMR and GCMS chromatograms of products were also given in supplementary Figures S_1-$S_3$and S_4-S_6 respectively.

Notably, utilization of the used Bi_2O_3 nanorods as catalyst in the second, third and fourth run aromatization reactions proceeded with 100% conversions with100% selectivities, respectively (Figure 7). Accordingly, the FT-IR spectrum of the recovered Bi_2O_3 nanorods (Figure 2e) was similar to the freshly prepared catalyst (Figure 2d). These evidences clearly indicate the reusability and stability of our prepared catalysis system.

Finally, the nanoparticles were also used under optimized reaction conditions. Compared to the catalytic activity of nanorods, similar activities were observed using 30 mg of the nanospecies as catalyst.

In comparison to the obtained results with those reported before, it was found that dihydropyridines have been aromatized to pyridines by various reagents as

Table 1. The effect of R group on aromatization of 1,4-DHP 's with Bi_2O_3 nanorods.[a]

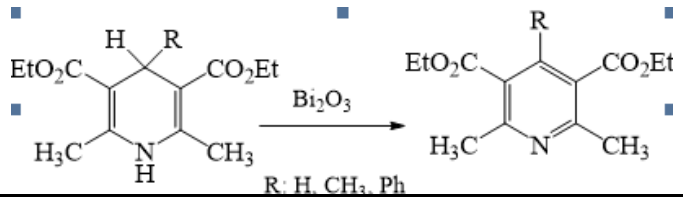

Entry	R	Time (h)	Amount of catalyst (mg)	Conversion (%)	Selectivity (%)
1	H	6	15	100	100
2		4	30	100	100
3	CH_3	8	15	100	100
4		6	30	100	100
5	Ph	24	15	72	100
6		8	30	100	100

[a]Conditions: substrate ; 20 mg (0.06 mmol), solvent ; ethanol, heated at reflux open to atmosphere.

Table 2. Oxidative aromatization of Hantzsch1,4-DHPs using different catalysts.

Catalyst	Oxidant	Time (min)	Yield (%)	Reference
SiO_2-$VO(OH)_2$	H_2O_2	60	50	[17]
K_2CO_3 (base)	-----	120	77	[18]
Silica supported cobalt	O_2	600	90	[19]
TiO_2/SiO_2	H_2O_2	300	96	[20]
Si-Zr-Mo	H_2O_2	3	100	[21]
MoO_3	H_2O_2	3	88	[22]
$MoCl_5$	------	3	93	[23]
$Ce(SO_4)_2 .4H_2O$	$O_{2(air)}$	10	98	[24]
Bi_2O_3	$O_{2\ (air)}$	480	100	current work[b]

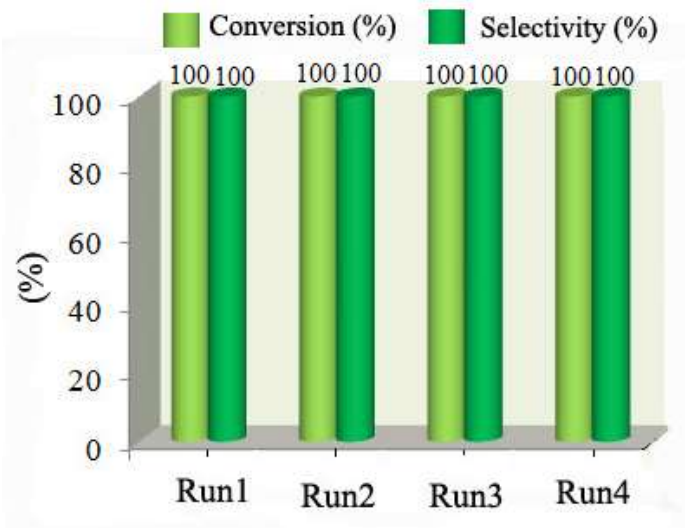

Figure 7. The reusability of catalyst on aromatization of 1,4-DHP.

shown in Table 2. Some of these methods need oxidants such as hydrogen peroxide or oxygen and longer reaction time. In fact these results indicated the unique Bi_2O_3 nanorods using as heterogeneous catalyst for Hantzsch oxidative aromatization of 1,4-DHPs to the corresponding substituted pyridines under air condition with high activity and selectivity is considerable.

Conclusion

In this study, Bi_2O_3 nanoparticles and nanorods were prepared in water under hydrothermal condition. The starch percentage as template was realized as determining factor on the product morphology due to the generation of Bi_2O_3 nanoparticles and nanorods at lower and higher template ratio, respectively. It was also found that the prepared nanorods catalyse the Hantzsch oxidative aromatization of 1,4-DHPs with 100% conversion and 100% selectivity.

Acknowledgements

The financial support from Alzahra University is gratefully acknowledged.

References

1. Zhang L., Hashimoto Y., Taishi T., Nakamura I. and Ni Q. Fabrication of Flower- Shaped Bi_2O_3 Superstructure by a Facile Template-Free Process, *Appl. Surf. Sci*. **257:** 6577-6582 (2011).
2. Gou X., Li R., Wang G., Chen Z. and Wexler D. Room-Temperature Solution Synthesis of Bi_2O_3 Nanowires for Gas Sensing Application. *Nanotechnology* **20:** 495-501(2009).
3. Li R., Chen W., Kobayashi H. and Ma C. Platinum-Nanoparticle-Loaded Bismuth Oxide: an Efficient Plasmonic Photocatalyst Active Under Visible Light. *Green Chem*. **12:** 212-215 (2010).
4. Gong Y., Ji W., Zhang L., Xie B. and Wang, H. Performance of (La,Sr)MnO_3 Cathode Based Solid Oxide Fuel Cells: Effect of Bbismuth Oxide Sintering Aid in Silver Paste Cathode Current Collector. *J. Power Sources* **196:** 928- 934(2011).
5. Malik P. and Chakraborty D. Bi_2O_3-Catalyzed Oxidation of Aldehydes with t-BuOOH *Tetrahedron Lett*. **51:** 3521-3523(2010).
6. Huang Q., Zhang, S., Cai C. and Zhou, B. Bi_2O_3/TiO_2

Coaxial Nanorods: Synthesis, Characterization and Photoluminescence Properties. *Thin Solid Films*, **518:** 6638- 6641(2010).
7. Anandan S. and Wu J.J. Microwave Assisted Rapid Synthesis of Bi_2O_3 Short Nanorods *Mater. Lett*. **63:** 2387- 2389 (2009).
8. Gujar T.P., Shinde V.R., Lokhande C.D., Mane R.S. and Han S.H. Formation of Highly Textured (1 1 1) Bi_2O_3 Films by Anodization of Electrodeposited Bismuth Films.
9. *Appl. Surf. Sci.* **252:** 2747- 2751(2006).
10. Gujar T.P., Shinde V.R. and Lokhande C.D. The Influence of Oxidation Temperature on Structural, Optical and Electrical Properties of Thermally Oxidized Bismuth Oxide Films. *Appl. Surf. Sci.* **254:** 4186- 4190 (2008).
11. Kim H. Jin C., Park S., Lee W. I., Chin I. J. and Lee C. Structure and Optical Properties of Bi_2S_3 and Bi_2O_3 Nanostructures Synthesized via Thermal Evaporation and
12. Thermal Oxidation Routes. *Chem. Eng. J*. **215:** 151- 156 (2013).
13. Lin G., Tan D, Luo F., Chen D., Zhao Q., Qiu J. and Xu Z. Fabrication and Photocatalytic Property of α-Bi_2O_3 Nanoparticles by Femtosecond Laser Ablation in Liquid. *J. Alloy. Comp*. **507:** L43- L46 (2010).
14. Weis F., Schneider R., Seipenbusch M. and Kasper G. Synthesis of Bi_2O_3/SiO_2 Core– Shell Nanoparticles by an Atmospheric CVS/CVD Process and Their Modification by Hydrogen or Electron-Beam induced reduction. *Surf. Coating Tech*. **230:** 93- 100 (2013).
15. Liao X., Lin W., Lu J. and Wang C. Oxidative Aromatization of Hantzsch 1,4- Ddihydropyridines by Sodium Chlorite. *Tetrahedron Lett*. **51:** 3859- 3861(2010).
16. Guenerich F.P., Brian W. R., Iwasak M., Sari M. A., Baarnheim C. and Berntsson P. Oxidation of Dihydropyridine Calcium Channel Blockers and Analogs by Human Liver Cytochrome P-450 IIIA4. *J. Med. Chem*.**34:** 1838- 1844(1991).
17. Heravi M.M., Oskooie H. A., Malakooti R., Alimadad B., Alinejad H. and Behbahani, F.K. Oxidative Aromatization of Hantzsch 1,4-Dihydropyridines in the Presence of a Catalytic Amount of $Mn(pbdo)_2Cl_2$/MCM-41 or $Mn(pbdo)_2Cl_2$/Al-MCM- 41 as Reusable and Green Catalysts. *Catal. Commun*. **10:** 819- 822 (2009).
18. Litvic M. F., Litvic M. and Vinkovic V. Rapid, Efficient, Room Temperature Aromatization of Hantzsch-1,4-Dihydropyridines with Vanadium(V) Salts: Superiority
19. of Classical Technique Versus Mmicrowave Promoted reaction. *Tetrahedron* 64: 10912- 10918 (2008).
20. Safaiee M., Zolfigol M. A., Tavasoli M. and Mokhlesi, M. Application of Silica Vanadic Acid [SiO_2-$VO(OH)_2$] as a Heterogeneous and Recyclable Catalyst for Oxidative Aromatization of Hantzsch 1,4-dihydropyridines at Room Temperature. *J. Iran Chem. Soc.* **11:** 1593-1597 (2014).
21. Shen L., Cao S., Wu J., Li H, Zhang J., Wu M. and Qian X. K_2CO_3-Assisted One- Pot Sequential Synthesis of 2-Trifluoromethyl- 6-Difluoromethylpyridine -3,5-icarboxylates Under Solvent-Free Conditions. *Tetrahedron Lett*. **51:** 4866- 4869 (2010).
22. Shamim T. Gupta M. and Paul S. The oxidative aromatization of Hantzsch 1,4- Dihydropyridines by Molecular Oxygen Using Surface Functionalized Silica Supported Cobalt Catalysts. *J. Mol. Catal. Chem. A* **302:** 15-19 (2009).
23. Angel L. M. S., Sathicq G., Thomas G. T. B. H. and Romanelli, G. P. Vanadium- Substituted Wells-Dawson Heteropolyacid as Catalyst for Liquid Phase Oxidation of 1,4- Dihydropyridine Derivative. *Catal. Lett*. 144: 172-180(2014).
24. Sharbatdaran M. Foruzin L. J., Farzaneh F. and Majd, M. L. Synthesis and Characterization of Si-Zr-Mo Nanocomposite as a Rapid and Efficient Catalyst for Aromatization of Hantzsch 1,4-dihydropyridines. *C. R. Chimie.* **16:** 176-182(2013).
25. Shahabi D., Amrollahi M. A. and Jafari A.A. NaI Readily Mediated Oxidative Aromatization of Hantzsch 1,4-Dihydropyridines with Hydrogen Peroxide at Room Temperature: A Green Procedure**.** *J. Iran Chem. Soc*. **8:** 1052- 1057(2011).
26. Litvic, M. Regovic, M. Šmic, K. Lovric, M. and Litvic, M. F. Remarkably fast and Selective Aromatization of Hantzsch Esters with $MoOCl_4$ and $MoCl_5$: A Chemical Model for Possible Biologically Relevant Properties of Molybdenum-Containing Enzymes, *Bioorg. Med. Chem. Lett.* **22:** 3676- 3681(2012).
27. Jia X., Yu L., Huo C., Wang Y. Liu J. and Wang, X. Catalytic Aromatization of 1,4- Dihydropyridines by Radical Cation Salt Prompted Aerobic Oxidation. *Tetrahedron Lett.* **55:** 264- 266 (2014).
28. Zolfigol M. and Safaiee M. Synthesis of 1,4-Dihydropyridines under Solvent-free Conditions, *Synlett.* **5:** 827- 828(2004).
29. Soest J. J. G. Hulleman S. H. D. Wit D. and Vliegenthart, J. F. G. Crystallinity in Starch Bioplastics. *Ind. Crop. Prod*. **5:** 11- 22(1996).
30. Yang X., Lian X. Liu S., Jiang C., Tian J., Wang G., Chen J. and Wang R. Visible Light Photoelectrochemical Properties of β-Bi_2O_3 Nanoporous Films: A Study of the
31. Dependence on Thermal Treatment and Film Thickness. *Appl. Surf. Sci*. **282:** 538- 543(2013).
32. Starches D. T. Jiang Q. Gao W. Li and Zhang X. J. Characteristics of Native and Enzymatically H ydrolyzed Zeamays. *Food Hydrocolloids* **25:** 521- 528(2011).
33. Abdullah E. A. Abdullah A. H. Zaina, Z. Husseni M. Z. and Ban T. K. Synthesis and Characterisation of Penta-Bismuth Hepta-Oxide Nitrate, Bi_5 O_7 NO_3, as a New Adsorbent for Methyl Orange Removal from an Aqueous Solution. *E-J. Chem*. **9:** 2429- 2438(2012).
34. Wang C. Shao C. Wang L. Zhang L., Li X. and Li Y. Electrospinning Preparation, Characterization and Photocatalytic Properties of Bi_2O_3 Nanofibers. *J. Colloid. Interface Sci.* **333:** 242- 248(2009).
35. Ma M.G., Zhu J.F. Sun R.C. and Zhu Y.J. Microwave-Assisted Synthesis of Hierarchical Bi_2O_3 Spheres Assembled from Nanosheets with Pore Structure. *Mater.Lett.* **64:** 1524- 1527(2010).